Braz J Phys (2013) 43:34–40
DOI 10.1007/s13538-013-0116-3

NUCLEAR PHYSICS

Description of Even–Even $^{114–134}$Xe Isotopes in the Transitional Region of IBM

M. A. Jafarizadeh · N. Fouladi · H. Sabri

Received: 1 May 2012 / Published online: 18 January 2013

Abstract Properties of $^{114–134}$Xe isotopes are studied in the *U(5)↔SO(6)* transitional region of Interacting Boson Model (IBM-1). The energy levels and *B(E2)* transition rates are calculated via the affine *SU*(1,1) Lie Algebra. The agreement with the most recent experimental is acceptable. The evaluated Hamiltonian control parameters suggest a spherical to γ-soft shape transition and propose the ^{130}Xe nucleus as the best candidate for the *E*(5) symmetry.

Keywords Interacting Boson Model (IBM) · Infinite dimensional algebra · Energy levels · *B(E2)* transition rates

1 Introduction

General algebraic group techniques, applied to the Interacting Boson Model (IBM), have rather successfully described the low-lying collective properties of a wide range of nuclei. In the relatively simple Hamiltonian of the model, the collective states are described by a system of interacting *s*- and *d*-bosons carrying angular momenta 0 and 2, respectively, which define an overall *U*(6) symmetry [1–5]. The IBM Hamiltonian has exact solutions in three dynamical symmetry limits [*U*(5), *O*(6), and *SU*(3)], which are geometrically analogous to the anharmonic vibrator, axial rotor and γ-unstable rotor, respectively. More generally, the Hamiltonian can be expressed in terms of an invariant operator of that chain of symmetries, and a shape phase transition between the dynamical symmetry limits results [6–8]. The analytic description of the structural change at the critical point of the phase transition being still an open problem, the Hamiltonian must be diagonalized numerically. Pan et al. [9], proposed a new solution based on the affine *SU*(1,1) algebraic technique, which determines the properties of nuclei in the *U(5)↔SO(6)* transitional region of IBM-1 [9, 10].

The xenon isotopes have been previously analyzed both theoretically and experimentally [11–29] with particular emphasis on describing the experimental data via collective models. The ground state properties of even–even Xe isotopes have been the subject to theoretical [11–20] and experimental studies [22] involving in-beam γ-ray spectroscopy. Recently, the nuclear structure of xenon isotopes have been investigated by Turkan in the IBM-1 model [30], while the energy levels, electric quadrupole moments and $B(E2)$ values of even-mass nuclei such as Ba,Xe were studied within the framework of the IBM-2 [19, 31–34]. These descriptions suggest these nuclei to be soft with regard to γ deformation with a nearly maximum effective triaxiality of $\gamma \cong 30°$ [11]. As pointed out by Zamfir et al. [11], Xe isotopes in the mass region $A \sim 130$ appear to evolve from *U*(5)-to *O*(6)-like structure in the IBM-1. It is very difficult to apply conventional mean-field theories to such structures, which are neither vibrational nor rotational.

Here we examine the even–even $^{114–134}$Xe isotopes in the *U(5)↔SO(6)* transition region and calculate the energy levels and $B(E2)$ transition probabilities in the frame work of IBM with the affine *SU*(1,1) algebraic technique. The estimated control parameters indicate a spherical to γ-soft shape

M. A. Jafarizadeh
Department of Theoretical Physics and Astrophysics, University of Tabriz, Tabriz 51664, Iran
e-mail: jafarizadeh@tabrizu.ac.ir

M. A. Jafarizadeh
Research Institute for Fundamental Sciences, Tabriz 51664, Iran

N. Fouladi · H. Sabri (✉)
Department of Nuclear Physics, University of Tabriz, Tabriz 51664, Iran
e-mail: h-sabri@tabrizu.ac.ir

transition. The same shape transition is revealed by the evolution of two-neutron separation energies S_{2n} [31] derived from experimental results [19, 32–34]. Also, special values are found for the ^{130}Xe control parameter and $R_{4/2}$, which suggest it as the best candidate for $E(5)$ dynamical symmetry in this isotopic chain.

This paper is organized as follows: Section 2 briefly summarizes the theoretical aspects of transitional Hamiltonian and the affine $SU(1,1)$ algebraic technique. Section 3 presents the numerical results obtained from applying the considered Hamiltonian to different isotopes. Finally, Section 4 summarizes our findings and the conclusions extracted from the results in Section 3.

2 Theoretical Framework

The phenomenological IBM in terms of *U(5)*, *O(6)* and *SU(3)* dynamical symmetries has been employed to describe the collective properties of several medium- and heavy-mass nuclei. These dynamical symmetries are geometrically analogous to the harmonic vibrator, axial rotor and γ-unstable rotor, respectively [1–5]. While these symmetries have already offered a fairly accurate description of the low-lying nuclear states, attempts to analytically describe the structure at the critical point of the phase transition have only been partially successful. Iachello [6, 7] established a new set of dynamical symmetries, i.e. $E(5)$ and $X(5)$, for nuclei located at critical point of transitional regions. The $E(5)$ symmetry, which describes a second-order phase transition, corresponds to the transitional states in the region from the $U(5)$ to the $O(6)$ symmetries in the IBM-1. Different analyses of this transitional region suggested certain nuclei, such as ^{134}Ba, ^{108}Pd, as examples of that symmetry [9, 14].

Elaborate numerical techniques are required to diagonalize the Hamiltonian in these transitional regions and critical points. To avoid these problems, an algebraic solution based on the affine $SU(1,1)$ Lie algebra has been proposed by Pan et al. [9, 10] to describe the properties of nuclei located in the *U(5)↔SO(6)* transitional region. The results of this approach are somewhat different from those obtained from the IBM, but as pointed out in Refs. [9, 10], there is a clear correspondence with the description of the geometrical model for this transitional region.

2.1 The Affine $SU(1,1)$ Approach to the Transitional Hamiltonian

References [9, 10] describe the $SU(1,1)$ algebra in detail. Here, we briefly outline the basic ansatz and summarize the results. The Lie algebra corresponding to the group $SU(1,1)$ is generated by the operators S^{ν}, $\nu=0$, and $\pm$, which satisfies the following commutation relations:

$$\left[S^0, S^{\pm}\right] = \pm S^{\pm} \quad , \quad \left[S^+, S^-\right] = -2S^0 \tag{2.1}$$

The Casimir operator of $SU(1,1)$ can be written as

$$\widehat{C}_2 = S^0\left(S^0 - 1\right) - S^+S^-, \tag{2.2}$$

Representations of $SU(1,1)$ are determined by a single number κ. The representation of the Hilbert space is hence spanned by orthonormal basis $|\kappa\mu\rangle$, where κ can be any positive number and $\mu=\kappa,\kappa+1,\ldots$. Therefore,

$$\widehat{C}_2(SU(1,1))|\kappa\mu\rangle = \kappa(\kappa-1)|\kappa\mu\rangle,\ S^0|\kappa\mu\rangle = \mu|\kappa\mu\rangle \tag{2.3}$$

The bases of $U(5)\supset SO(5)$ and $SO(6)\supset SO(5)$ are simultaneously the bases of $SU^d(1,1)\supset U(1)$ and $SU^{sd}(1,1)\supset U(1)$, respectively. For $U(5)\supset SO(5)$ case, one has

$$\begin{aligned}&|Nn_d\nu n_\Delta LM\rangle \\ &= \left|N, \kappa^d = \frac{1}{2}\left(\nu+\frac{5}{2}\right), \mu^d = \frac{1}{2}\left(n_d+\frac{5}{2}\right), n_\Delta LM\right\rangle,\end{aligned} \tag{2.4}$$

Where N, n_d, ν, L and M are quantum numbers of *U(6)*, *U(5)*, *SO(5)*, *SO(3)*, and *SO(2)*, respectively, while n_Δ is an additional quantum number needed in the reduction *SO(5)↓SO(3)* and κ^d and μ^d are quantum numbers of $SU^d(1,1)$ and *U(1)*, respectively. On the other hand, in the IBM-1, the generators of the d-boson pairing algebra created by

$$\begin{aligned}&S^+(d) = \frac{1}{2}\left(d^\dagger.\, d^\dagger\right) \quad , \quad S^-(d) = \frac{1}{2}\left(\widetilde{d}.\widetilde{d}\right) \quad , \\ &S^0(d) = \frac{1}{4}\sum_\nu\left(d_\nu^\dagger d_\nu + d_\nu d_\nu^\dagger\right)\end{aligned} \tag{2.5}$$

Similarly, the s-boson pairing forms another $SU^s(1,1)$ algebra generated by the operators

$$\begin{aligned}&S^+(s) = \frac{1}{2}s^{\dagger 2} \quad , \quad S^-(s) = \frac{1}{2}s^2 \quad , \\ &S^0(s) = \frac{1}{4}\left(s^\dagger s + ss^\dagger\right)\end{aligned} \tag{2.6}$$

The infinite dimensional $SU(1,1)$ algebra is then generated by the operators [9, 10]

$$S_n^{\pm} = c_s^{2n+1} S^{\pm}(s) + c_d^{2n+1} S^{\pm}(d) \quad ,$$
$$S_n^0 = c_s^{2n} S^0(s) + c_d^{2n} S^0(d) \tag{2.7}$$

where C_s and C_d are real parameters and n can be 0,± 1,±2,….

The generators in Eq. (2.7) satisfy the commutation relations

$$\left[S_m^0, S_n^{\pm}\right] = \pm S_{m+n}^{\pm} \quad , \quad \left[S_m^+, S_n^-\right] = -2S_{m+n+1}^0 \tag{2.8}$$

It follows that the $\{S_m{}^{\mu}, \mu=0,+,-;\pm1,\pm2,\ldots\}$ generate an affine Lie algebra $\widehat{SU(1,1)}$ without central extension. From the generators of the Algebra, the following Hamiltonian for transitional region between *U(5)↔SO(6)* limits can then be written [9, 10]

$$\widehat{H} = g\ S_0^+ S_0^- + \varepsilon\ S_1^0 + \gamma\ \widehat{C}_2(SO(5)) + \delta\ \widehat{C}_2(SO(3)) \tag{2.9}$$

g, ε, γ and δ are real parameters and $\hat{C}_2(SO(3))$ and $\hat{C}_2(SO(5))$ denote the Casimir operators of these groups. It can be seen that the Hamiltonian (Eq. 2.9), would be equivalent with the *SO(6)* Hamiltonian if c_s=c_d and to the *U(5)* Hamiltonian if c_s=0 & c_d≠0. Therefore, the inequalities c_s≠c_d≠0 correspond to the *U(5)↔SO(6)* transitional region. In our calculation, we let c_d be a constant(=1) and c_s vary between 0 and c_d.

In order to obtain the eigenstates of the Hamiltonian (Eq. 2.9), we exploit a Fourier–Laurent expansion of the eigenstates and the generators in terms of unknown *c*-number parameters *Xi (i= 1, 2, ..., k)*; in other words, we write the eigenstates in the form [9, 10]

$$|k; v_s v n_\Delta L M\rangle = \sum_{n_i \in Z} a_{n_1} a_{n_2} \ldots a_{n_k} x_1^{n_1} x_2^{n_2} \ldots x_k^{n_k} S_{n_1}^+ S_{n_2}^+ \ldots S_{n_k}^+ |lw\rangle, \tag{2.10}$$

Given the analytical behavior of the wavefunctions, it suffices to consider X_i near zero. The commutation relations (Eq. 2.1) between the generators of *SU(1,1)* algebra (Eq. 2.3), the allow us to express the wavefunctions as:

$$|k; v_s v n_\Delta L M\rangle = N S_{x_1}^+ S_{x_2}^+ \ldots S_{x_k}^+ |lw\rangle, \tag{2.11}$$

Where N is a normalization factor and

$$S_{x_i}^+ = \frac{c_s}{1 - c_s^2 x_i} S^+(s) + \frac{c_d}{1 - c_d^2 x_i} S^+(d), \tag{2.12}$$

The *c*-numbers x_i are determined by the following set of equations (v_s denotes the quantum number of *SO(5)* group for *s* bosons)

$$\frac{\varepsilon}{x_i} = \frac{g c_s{}^2 \left(v_s + \frac{1}{2}\right)}{1 - c_s{}^2 x_i} + \frac{g c_d^2 \left(v + \frac{5}{2}\right)}{1 - c_d^2 x_i} - \sum_{i \neq j} \frac{2}{x_i - x_j} \quad \text{for} \quad i = 1, 2, \ldots, k \tag{2.13}$$

The eigenvalues $E^{(k)}$ of Hamiltonian (Eq. 2.9) can be expressed in the form [9, 10]

$$E^{(k)} = h^{(k)} + \gamma v(v+3) + \delta L(L+1) + \varepsilon \Lambda_1^0 \quad ,$$
$$\Lambda_1^0 = \frac{1}{2}\left[c_s^2\left(v_s + \frac{1}{2}\right) + c_d^2\left(v + \frac{5}{2}\right)\right] \tag{2.14}$$

where

$$h^{(k)} = \sum_{i=1}^{k} \frac{\varepsilon}{x_i}, \tag{2.15}$$

The quantum number k is related to the total boson number by the equality

$$N = 2k + v_s + v$$

To obtain numerical results for $E^{(k)}$(energy spectra of considered nuclei), we have followed the prescriptions introduced in Refs. [9, 10], i.e., we have solved a set of nonlinear Bethe ansatz equations with k unknowns for k pair excitations. It is convenient to change variables as follows

$$\varepsilon = \frac{\varepsilon}{g} g = 1\ \textit{ke v}[7-8]) \qquad c = \frac{c_s}{c_d} \leq 1 \qquad y_i = c_d^2 x_i$$

to rewrite Eq. (2.13) in the form

$$\frac{\varepsilon}{y_i} = \frac{c^2\left(v_s + \frac{1}{2}\right)}{1 - c^2 y_i} + \frac{\left(v + \frac{5}{2}\right)}{1 - y_i} - \sum_{i \neq j} \frac{2}{y_i - y_j} \quad \text{for} \quad i = 1, 2, \ldots, k \tag{2.16}$$

To determine the roots of the Bethe ansatz equations with specified values of v_s and v, we solve Eq. (2.16) with definite values of c and ε for i=1 and then use the function "Find root" in Maple13 to obtain all y_j's. We then repeat this procedure with different c and ε to minimize the deviation σ between the energy spectra (after inserting γ and δ) and the experimental values. The deviation is defined by the equality

$$\sigma = \left(\frac{1}{N_{tot}} \sum_{i,tot} \left|E_{\exp}(i) - E_{cal}(i)\right|^2\right)^{1/2}$$

where N_{tot} is the number of energy levels in the fit. To optimize the set of Hamiltonian parameters γ and δ, we have carried out a least-square fit to the available experimental

data [35–38] of the excitation energies for selected states, 0_1^+, 2_1^+, 4_1^+, 0_2^+, 2_2^+, 4_2^+, etc. (12 levels up to 2_4^+, although not all of them are available for all considered nuclei) or of the two-neutron separation energies of considered nuclei.

2.2 *B(E2)* Transition

Additional information on the structure of nuclei can be obtained from other observables: the reduced electric quadrupole transition probabilities *B(E2)* and quadrupole moment ratios within the low-lying. The E2 transition operator must be a Hermitian tensor of rank two; consequently, the number of bosons must be conserved. These constraints limit to two the number of allowed in lowest order, the electric quadrupole transition operator being given by the expression [9],

$$\widehat{T}_{\mu}^{(E2)} = q_2\left[\widehat{d}^{\dagger}\times\widetilde{s}+\widehat{s}^{\dagger}\times\widetilde{d}\right]_{\mu}^{(2)}+q_2^{'}\left[\widehat{d}^{\dagger}\times\widetilde{d}\right]_{\mu}^{(2)}, \qquad (2.17)$$

Where q_2 is the effective quadrupole charge, $q_2^{'}$ is a dimensionless coefficient, and $s^{\dagger}(d^{\dagger})$ is the creation operator of *s(d)* boson. The reduced electric quadrupole transition rates between $I_i \rightarrow I_f$ states are given by [5]

$$B\left(E2; I_i \rightarrow I_f\right) = \frac{\left|\left\langle I_f \| T(E2) \| I_i \right\rangle\right|}{2I_i+1}, \qquad (2.18)$$

To determine the q_2 and $q_2^{'}$, we have followed the procedure in Refs. [9, 10], i.e. treated these parameters as function of total boson number *N*.

3 Numerical Result

3.1 Energy Levels

The experimental energy spectra [11–22], suggest that we collect empirical evidence concerning the *U(5)↔SO(6)* transitional region from $^{114-134}$Xe isotopes. We have, therefore computed the energy spectra for the transition-region Hamiltonian of Eq. (2.9). Figure 1 displays 12 levels, up to 2_4^+, for an illustrative set of nuclei in our fitting procedure. Table 1 shows the optimal Hamiltonian parameters ε, c_s, δ, and γ resulting from the procedure in Section 2, i.e., the parameters minimizing the deviation σ calculated from the experimental data in Refs. [38–41]. Shown in Fig. 1 are the available experimental levels and corresponding calculated levels for ^{120}Xe–^{126}Xe isotopes in the low-lying region of the spectra. The agreement is acceptable.

3.2 Transition Probabilities

The stable even–even nuclei in Xe isotopic chain offer an excellent opportunity to study the behavior of the total low-lying E2 strengths in the transitional region from deformed to spherical nuclei. The computation of the electromagnetic transition probabilities provides a reliable test of the nuclear-model wave functions. To determine the boson effective charges q_2 and q'_2, we fit the theoretical results to the empirical *B(E2)* values, taking the two parameters to be function of the total boson number *N* [9, 10]. The theoretical *B(E2)* transition rates, which are displayed in Fig. 2, are associated with the effective charge parameters in Table 2.

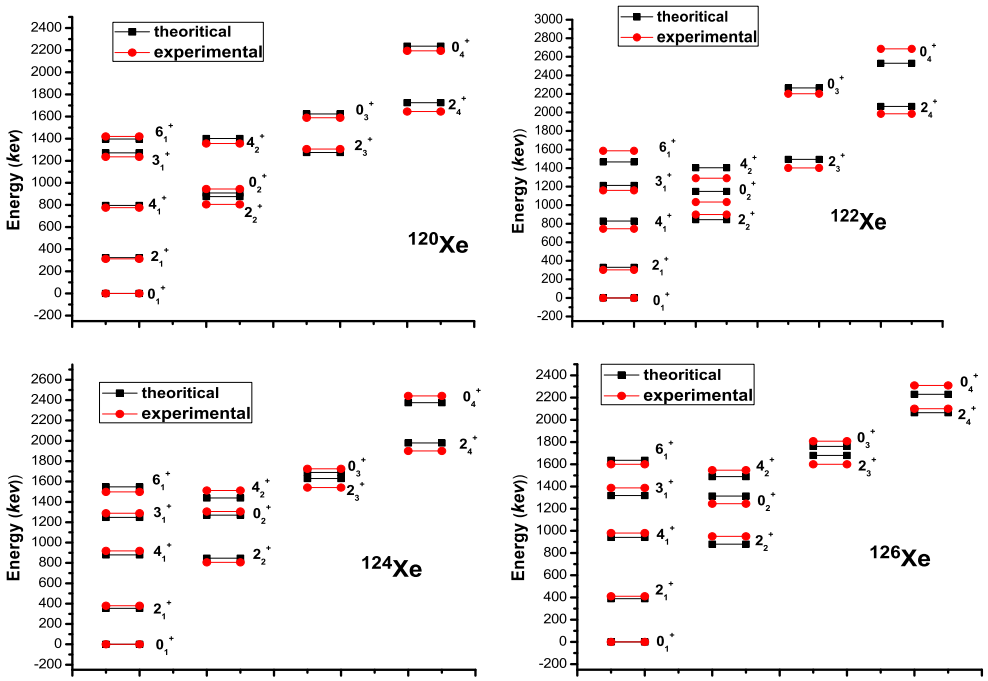

Fig. 1 Comparison of calculated energy levels and experimental spectra taken from Refs. [35–38] for $^{120-126}$Xe isotopes. Due to similar correspondences, we do not present this comparison for other isotopes

Table 1 The parameters of the Hamiltonian (Eq. 2.9) determined by least-square fitting to the experimental data for different *Xe* isotopes. N is the boson number and ε, c_s, γ and δ are the parameters of transitional Hamiltonian (Eq. 2.9) for each nuclei. The deviation σ monitors the quality of the fitting

Nucleus	N	ε(kev)	c_s	γ(kev)	δ(kev)	σ
$^{114}_{54}$Xe	7	800	0.66	54.83	−60.01	151
$^{116}_{54}$Xe	8	1430	0.59	21.44	−56.87	112
$^{118}_{54}$Xe	9	755	0.79	−52.87	39.10	89
$^{120}_{54}$Xe	10	620	0.86	−45.96	41.24	104
$^{122}_{54}$Xe	9	540	0.95	−29.64	30.90	68
$^{124}_{54}$Xe	8	680	0.89	−61.36	43.36	75
$^{126}_{54}$Xe	7	695	0.83	−56.05	43.77	91
$^{128}_{54}$Xe	6	1570	0.65	−138.83	43.11	88
$^{130}_{54}$Xe	5	1100	0.46	−79.58	39.71	105
$^{132}_{54}$Xe	4	1680	0.37	−114.77	40.31	115
$^{134}_{54}$Xe	3	670	0.06	1.85	20.14	73

Figure 2 compares our results for $B\left(E2; 2_1^+ \rightarrow 0_1^+\right)$, $B(E2; 4_1^+ \rightarrow 2_1^+)$ and the ratio $B\left(E2;\ 4_1^+ \rightarrow 2_1^+\right)/B\left(E2;\ 2_1^+ \rightarrow 0_1^+\right)$

Table 2 Coefficients q_2 and q_2' resulting from our analysis, similar to the procedure in Refs. [9, 10]. The corresponding *B(E2)* values are compared to the experimental data in Fig. 2

Nucleus	q_2	q_2'	Nucleus	q_2	q_2'
$^{114}_{54}$Xe	0.136	−0.335	$^{116}_{54}$Xe	0.148	−0.415
$^{118}_{54}$Xe	0.154	−0.515	$^{120}_{54}$Xe	0.164	−0.637
$^{122}_{54}$Xe	0.149	−0.502	$^{124}_{54}$Xe	0.141	−0.398
$^{126}_{54}$Xe	0.133	−0.324	$^{128}_{54}$Xe	0.128	−0.271
$^{130}_{54}$Xe	0.121	−0.219	$^{132}_{54}$Xe	0.113	−0.176
$^{134}_{54}$Xe	0.106	−0.143			

with experimental values [35–38]. In all figures in this paper, the experimental uncertainties are smaller than the symbols. The good agreements in Figs. 1 and 2 attest to the reliability of the fitting procedure and of our computation of the *B(E2)* transition probabilities of even–even Xe isotopes, respectively. The control parameters in Table 1 moreover provide information on the structural changes in nuclear deformation and shape phase transition.

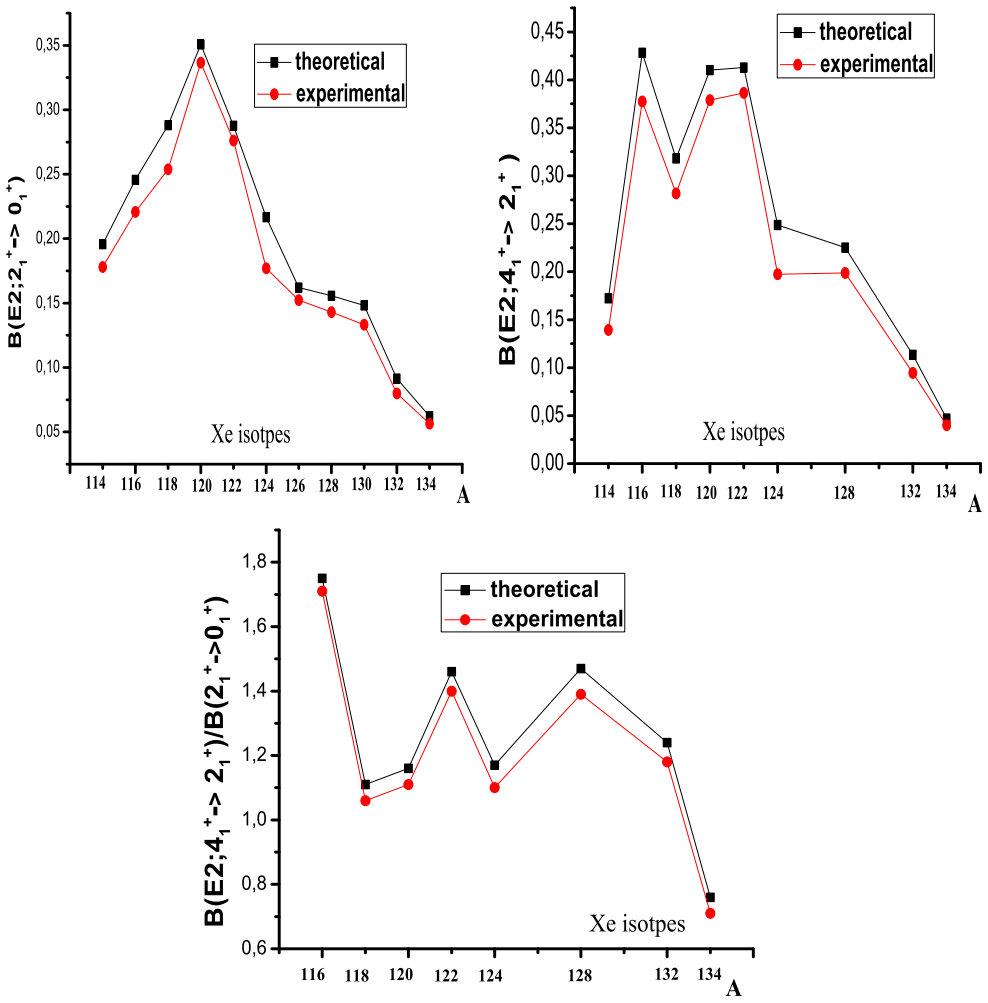

Fig. 2 Comparison of calculated transition probabilities and corresponding experimental values taken from Refs. [35–38]. $B(E2;2_1^+ \rightarrow 0_1^+)$ for $^{114-134}$Xe isotopes, $B(E2; 4_1^+ \rightarrow 2_1^+)$ for $^{114\text{-}134}$Xe except (^{126,130}Xe). The figure also indicates the calculated $B_{4/2}$ ratios and experimental ones for $^{114-134}$Xe except (^{114,126,130}Xe) nuclei

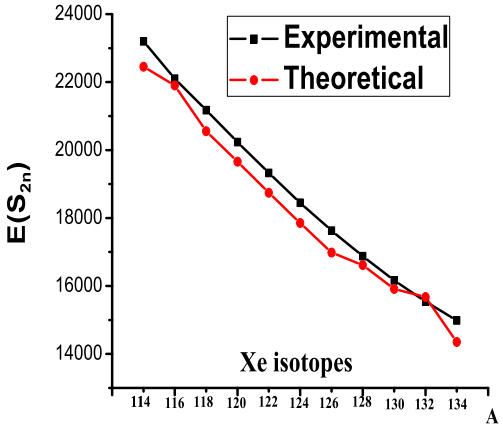

Fig. 3 Experimental and theoretical S_{2n} energies (in *kev*) for considered nuclei

The ground state two-neutron separation energies S_{2n} are sensitive to the details of nuclear structure. Gross nuclear structure features, such as major shell closures, are clearly seen in the evolution of this observable along the isotopic chains [39–41]. Zamfir et al. [40] have suggested that S_{2n} vary smoothly as the nuclei undergo a second-order shape phase transition between spherical (*U(5)*) and γ-unstable rotor *(SO (6))* limits. The correlations between the two observables, one S_{2n} related to ground state properties and other, $R_{4/2}$, related to the properties of the excited states, is a convenient probe of the shape phase transition region. In order to bring to light the nuclear structure information in the two observables, we studied the evolution of the two-neutron separation energies *(S_{2n})* along the isotopic chains for the even–even Xe nuclei. Experimental and theoretical values are presented in Fig. 3, including the last review of nuclear masses in Ref. [37] and the most recent available data [35–38]. On the theoretical side, to determine S_{2n} in the framework of the IBM-1, we have followed the prescription in Ref. [36]. According to Iachello's definition, as a function of proton and neutron number, the binding energy is given by [39]

$$E_B(N_p,N_n) = E^{(c)} + A_pN_p + A_nN_n + \frac{1}{2}B_pN_p(N_p-1) + \frac{1}{2}B_nN_n(N_n-1) + CN_pN_n + \widetilde{E}(N_p,N_n), \tag{3.1}$$

where $N_p(N_n)$ is the number of proton(neutron) bosons in the valence shell, $E^{(c)}$ the contribution from the core and $\tilde{E}$ is the contribution to the binding energy due to the deformation. Using the Eq. (3.1), one obtains the following relation for the two neutron separation energy

$$\begin{aligned} S_{2n}(N_p,N_n) &= E_B(N_p,N_n) - E_B(N_p,N_n-1) \\ &= A_n + BN_p + C_nN_n \\ &\quad + \left[\widetilde{E}(N_p,N_n) - \widetilde{E}(N_p,N_n-1)\right], \end{aligned} \tag{3.2}$$

The Xe isotopes have N_p=2 but different numbers of neutron bosons. Letting A_n+B=23.70*Mev* and C_n= 0.814 Mev, we obtain the two neutron separation energies compared with experimental values in Fig. 3, which shows good agreement. The results confirm the predictions by Zamfir et al. and suggest that the phase transition for this chain of Xe isotopes is of second order.

The shape phase transition is associated with a sudden change in nuclear collective behavior, as a result of which the ratio $R_{4/2} = E_{4_1^+}\big/E_{2_1^+}$ suddenly increases, from the spherical vibrator value of 2.0 to the deformed γ-soft nuclei value of 2.5. Iachello proposed the value 2.20 for the *E(5)* dynamical symmetry characterizing the critical point of *U (5)↔SO(6)* transitional region [7]. Table 3 shows the estimated control parameters c_s and the ratio $R_{4/2}$ for the isotopic chain. The evolution of these quantities between spherical (c_s=0&$R_{4/2}$=2.0 for the *U(5)* limit) and γ-unstable (c_s=1&$R_{4/2}$=2.5 for the *SO(6)* limit) shapes, are in line with the second-order shape phase transition highlighted in our discussion of Fig. 3.

The variation of the control parameters, $c_s \sim 0 \rightarrow 1$, indicates structural changes in nuclear deformation and shape phase transitions in even–even $^{114-134}$Xe isotopes. Iachello took n to be the control parameter in his description of the shape phase transition [6], so that the critical points of the transitional regions are expected at or near $n=0.5$. By the same token, we expect the *E(5)* symmetry to arise at or near $c_s=0.5$ in our approach. The control parameters and ratios in Table 3 give evidence favoring the notion of *E(5)* symmetry for ^{130}Xe [42, 43], which displays values of c_s and $R_{4/2}$ that come closest to Iachello's prediction, $R_{4/2}\sim$2.24 and $c_s\sim$0.46.

Table 3 Control parameters c_s and $R_{4/2}$ ratio for the considered nuclei. The special values of the two parameters identify ^{130}Xe as the best candidate for *E(5)* dynamical symmetry

Nuclei	$^{114}_{54}$Xe	$^{116}_{54}$Xe	$^{118}_{54}$Xe	$^{120}_{54}$Xe	$^{122}_{54}$Xe	$^{124}_{54}$Xe	$^{126}_{54}$Xe	$^{128}_{54}$Xe	$^{130}_{54}$Xe	$^{132}_{54}$Xe	$^{134}_{54}$Xe
c_s	0.66	0.59	0.79	0.86	0.95	0.89	0.83	0.65	0.46	0.37	0.06
$R_{4/2}nE$	2.38	2.33	2.40	2.47	2.50	2.48	2.42	2.33	2.24	2.15	2.02

4 Conclusions

We have employed an affine *SU(1,1)* Lie algebra to calculate the energies and *B(E2)* transition probabilities for the $^{114-134}$Xe nuclei within the framework of the Interacting Boson Model. We have checked the validity of the parameters chosen in our formulation of the IBM-1 Hamiltonian and found satisfactory agreement between the presented and experimental data. Our study accounts for the general characteristics of the Xe isotopes and support the notion of shape coexistence. Figures 1, 2, and 3 show acceptable agreement between the presented IBM-1 results and the experimental results for the considered nuclei. The Xe being close to both proton and neutron closed shells, these nuclei are not expected to be deformed. Gamma-soft rotor features exist in Xe isotopes but the vibrational character is dominant. Our results confirm the adequacy of the method to describe the structure of nuclei around mass $A \sim 130$.

References

1. F. Iachello, A. Arima, *The Interacting Boson Model* (Cambridge University Press, Cambridge, 1987)
2. A. Arima and F. Iachello, Ann. Phys.(N.Y.) 99 (1976) 253
3. A. Arima and F. Iachello, Ann. Phys. (N.Y.) 111 (1978)201
4. A. Arima and F. Iachello, Ann. Phys.(N.Y.) 123 (1979) 468
5. R.F. Casten, D.D. Warner, Rev. Mod. Phys. **60**, 389 (1988)
6. F. Iachello, Phys. Rev. Lett. **87**, 052502 (2001)
7. F. Iachello, Phys. Rev. Lett. **85**, 3580 (2000)
8. P. Cejnar, J. Jolie, R.F. Casten, Rev. Mod. Phys. **82**, 2155 (2010)
9. J.P. Feng Pan, Draayer NuclPhys A. **636**, 156 (1998)
10. J.P. Feng Pan, J. Draayer, Phys A: Math. Gen. **35**, 7173 (2002)
11. N.V. Zamfir, W.T. Chou, R.F. Casten, Phys. Rev. C. **57**, 427 (1998)
12. T. Otsuka, Nucl. Phys. A. **557**, 531 (1993)
13. B. Saha et al., Phys. Rev. C. **70**, 034313 (2004)
14. W. Lieberz, A. Dewald, W. Frank, A. Gelberg, W. Krips, D. Lieberz, R. Wirowski, P. Von Brentano Phys, LettB. **240**, 38 (1990)
15. F. Seiffert, W. Lieberz, A. Dewald, S. Freund, A. Gelberg, A. Granderath, D. Lieberz, R. Wirowski, P. von Brentano, Nucl. Phys. A. **554**, 287 (1993)
16. R. Wyss et al., Nucl. Phys. A. **505**, 337 (1989)
17. U. Meyer, A. Faessler, S.B. Khadkikar, Nucl. Phys. A. **624**, 391 (1997)
18. A. Sevrin, K. Heyde, J. Jolie, Phys. Rev. C. **36**, 2631 (1987)
19. P.F. Mantica Jr., B.E. Zimmerman, W.B. Walters, J. Rikovska, N.J. Stone, Phys. Rev. C. **45**, 1586 (1992)
20. M.T.F. da Cruz, I.D. Goldman, Phys. Rev. C. **42**, 869 (1990)
21. B. Singh, R. Iafigliola, K. Sofia, J.E. Crawford, J.K.P. Lee, Phys. Rev. C. **19**, 2409 (1979)
22. C. Girit, W.D. Hamilton, E. Michelakakis, J. Phys. G: Nucl. Phys. **6**, 1025 (1980)
23. L. Goettig, C.H. Droste, A. Dygo, T. Morek, J. Srebrny, R. Broda, J. Stycze, J. Hattula, H. Helppi, M. Jääskeläinen, Nucl.Phys. A. **109** (1981)
24. W. Gast, U. Kaup, H. Hanewinkel, R. Reinhardt, K. Schiffer, K.P. Schmittgen, K.O. Zell, J. Wrzesinski, A. Gelberg, P.V. Brentano, Z. Phys. A. **318**, 123 (1984)
25. R. Reinhardt, A. Dewald, A. Gelberg, W. Lieberz, K. Schiffer, K.P. Schmittgen, K.O. Zell, P. Von Brentano, Z. Phys. A. **329**, 507 (1988)
26. D. Jerrestam, S. Elfström, W. Klamra, T. Lindblad, C.G. Lindén, V. Barci, H. El-Samman, J. Gizon, Nucl. Phys. A. **481**, 355 (1988)
27. P. Von Brentano, A. Gelberg, S. Harissopulos, R.F. Casten, Phys. Rev. C. **38**, 2386 (1988)
28. Y.A. Luo, J.Q. Chen, J.P. Draayer, Nucl. Phys. A. **669**, 101 (2000)
29. D.J. Rowe, Phys. Rev. Lett. **93**, 122502 (2004)
30. N. Turkan, J. Phys. G: Nucl. Part. Phys. **34**, 2235 (2007)
31. T. Otsuka, HYPERFINE INTERACTIONS **74**, 93 (1992)
32. A. Gade, I. Wiedenhover, J. Gableske, A. Gelberg, H. Meise, N. Pietralla, P. von Brentano, Nucl.Phys.A. **665**, 268 (2000)
33. L.I. Zhong Ze, L.I.U. FengYing, J.I. HuaYing, Z. JinFu, P. JaeYon, Commun. Theor. Phys. **83**, 593 (2000)
34. I. Maras, R. Gumus, N. Turkan, Mathematical and Computational Applications **15**, 79 (2010)
35. National Nuclear Data Center, (Brookhaven National laboratory), chart of nuclides, (http://www.nndc.bnl.gov/chart/reColor.jsp?newColor=dm)
36. Live chart, Table of Nuclides, (http://www-nds.iaea.org/relnsd/vcharthtml/VChartHTML.html).
37. Richard B. Firestone, Virginia S. Shirley, S.Y. Frank, Coral M. Baglin and Jean Zipkin, table of isotopes, (1996).
38. P. Möller, J.R. Nix, W.D. Myers, W.J. Swiatecki, At. Data. Nucl. Data Tables. **59**, 185 (1995)
39. F. Iachello, A. Arima, Phys. Rev. C. **16**, 2085 (1977)
40. N.V. Zamfir, S. Anghel, G. Cata-Danil, AIP Conf. Proc. 1072 (2008)118
41. A.E.L. Dieperink, O. Scholten, F. Iachello, Phys. Rev. Lett. **44**, 1744 (1980)
42. D.A.-l. Zhang, L. Yu-Xin, Chin.Phys.Lett. **20**, 1028 (2003)
43. R.M. Clark et al., Phys.Rev.C. **69**, 064322 (2004)